ELSEVIER

Journal of Molecular Structure (Theochem) 506 (2000) 191–211

THEO CHEM

www.elsevier.nl/locate/theochem

Structure and stability of enediynes containing heteroatoms—a quantum chemical investigation ☆

E. Kraka*, D. Cremer

Department of Theoretical Chemistry, Göteborg University, Reutersgatan 2, S-41320 Göteborg, Sweden

Abstract

Structure and stability of 12 enediynes containing N and being potential candidates for the design of new antitumor drugs are investigated at the B3LYP/6-31G(d,p) level of theory using (*Z*)-hex-3-ene-1,5-diyne (**1**) and more than 30 alkenes, alkines, amides, amidines, and cumulenes as appropriate reference molecules. **1** is found to be stabilized by 18 kcal/mol due to π-delocalization. Incorporation of a N atom in position 3 of **1** destabilizes the enediyne because of a reduction of π delocalization while incorporation of the N atom in a terminal position strongly stabilizes the enediyne, and by this it is no longer useful as a starting point for the design of a new antitumor drug. Heterocumulenes are also not useful since they easily rearrange to more stable molecules. The most promising candidates for new antitumor drugs are amidines possessing two ethinyl substituents. They can be easily protonated in the weakly acidic medium of the tumor cell and should rearrange to produce biologically active biradicals.

Keywords: Hetero-enediynes; Structure; Stability; DFT calculations

1. Introduction

Enediynes represent an important class of biochemically interesting compounds since naturally occurring enediynes have been found to be strong antibiotics and starting compounds for the design of new antitumor drugs [1–8]. Work of the last ten years has primarily focused on the derivatives of (*Z*)-hex-3-ene-1,5-diyne (**1a**, see Scheme 1), which by Bergman cyclization [9–15] forms the biologically active *para*-didehydrobenzene biradical [16–18]. Only recently, research was extended to the first enediyne containing an heteroatom, namely (*Z*)-3-aza-hex-3-ene-1,5-diyne (**2**, Scheme 1) [19]. Enediyne **2** leads to the 2,5-didehydropyridine biradical, which can also be formed by cyclization of the nitrile **3** of Scheme 1 as **2** and **3** are isomers. Compound (**2**) can be protonated in the weakly acidic medium of the tumor cell to yield **4**, which after Bergman reaction generates the corresponding 2,5-didehydropyridinium biradical, which is supposed to be more active than the 2,5-didehydropyridine biradical [19].

Quantum chemical investigations have considerably improved knowledge about enediyne **1** and its derivatives [16,20–27]. Some calculational studies have also been carried out for **2** since there is a need to understand the biological activity of hetero-enediynes [28]. As an alternative to **2**, which bear some disadvantages, amides such as **6** were suggested [19], however no investigation was attempted so far. In recent work, we have pointed out that amidines such as **10** might actually be better candidates for antitumor drugs [29]. Since there is a strong interest in N-containing enediynes, we investigate in this work

☆ Presented at the 5th World Congress of Theoretically Oriented Chemists (WATOC), Imperial College, London, 1–6 August, 1999.

* Corresponding author.

0166-1280/00/$ - see front matter
PII: S0166-1280(00)00412-7

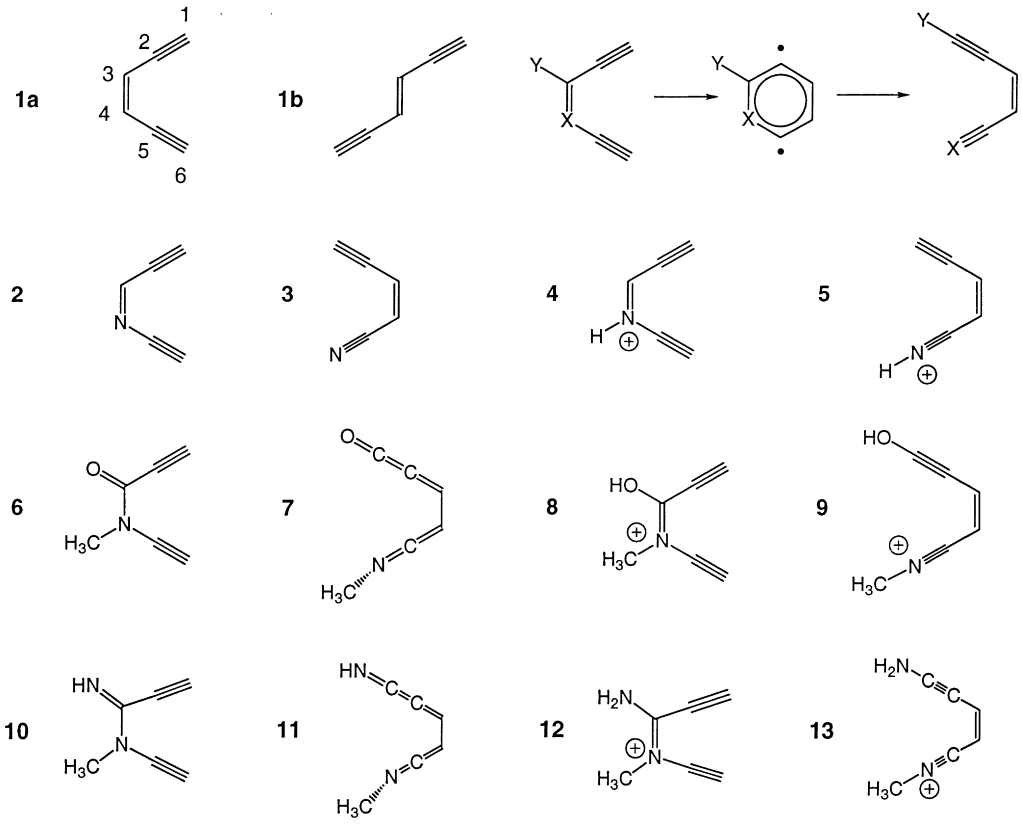

Scheme 1.

enediynes **2**–**13** shown in Scheme 1. Enediynes **2**–**13** are given in their *Z* form as this is the starting point of the Bergman cyclization reaction. (*E*)-hex-3-ene-1,5-diyne **1b** should be more stable than (*Z*)-hex-3-ene-1,5-diyne **1a**, however **1b** has no biological activity as it does not form the *para*-didehydrobenzene biradical via Bergman reaction. Therefore, no other *E* form was investigated in this work. Enediynes **2**–**13** are related either by isomerization (**2** and **3**, **4** and **5**, **6** and **7**, **8** and **9**, **10** and **11**, **12** and **13**) or by protonation (**2** and **4**, **3** and **5**, **6** and **8**, **7** and **9**, **10** and **12**, **11** and **13**) where the protonated forms are of particular interest since they could be formed in the tumor cell. Isomerization must involve a Bergman and a retro-Bergman cyclization step as is indicated in the reaction of Scheme 1.

While for the isomeric pair **2**–**3** and all the protonated molecules the enediyne structure is apparent despite N atom and substituents, molecules **6**, **7**, **10**, and **11** have different structures, which may be described as amide (**6**), amidine (**10**), oxocumulene (**7**), and azacumulene (**11**). Scheme 1 reveals that despite the difference between pairs **2**/**3**, **6**/**7**, and **10**/**11**, the protonated enediynes formally form two groups of closely related enediynes, namely **4**, **8**, and **12** as well as **5**, **9**, and **13**. All compounds can form a highly reactive singlet biradical via Bergman cyclization, which will become obvious if one considers their (mesomeric) zwitterionic forms shown in Scheme 2. Therefore, we will address molecules **6**, **7**, **10**, and **11** as enediynes, but we will alternatively also point to their amide, amidine or cumulene nature. Calculations have to clarify whether the zwitterionic structures of Scheme 2 influence the properties of **6**, **7**, **10**, and **11** in their equilibrium geometries. Reversibly, we will check whether molecules **9** and **13** are primarily protonated enediynes or can also possess some cumulene nature.

This investigation focuses on the structure and

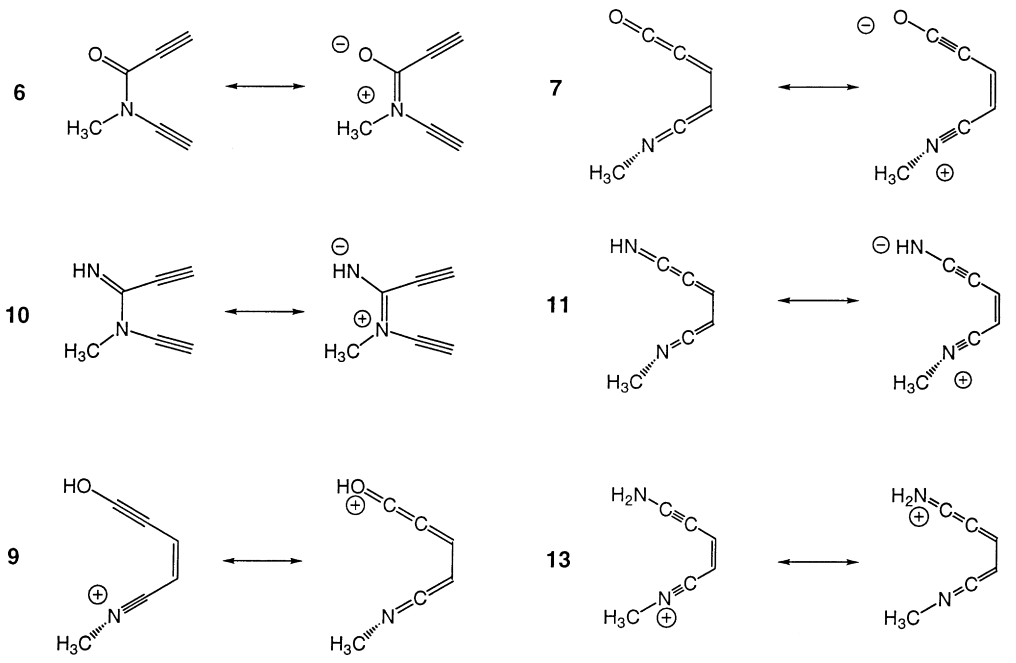

Scheme 2.

stability of enediynes **2**–**13** using the parent molecule **1** as suitable reference. In addition, we will investigate formal reactions, which are used to compare **1**–**13** with smaller reference molecules containing structural units of an enediyne. In this way, we will assess the energetic consequences of π-delocalization, bond–bond interactions, and through–space interactions active in enediynes. The reference molecules **14**–**41**, which had to be calculated for this purpose, are shown in Scheme 3. Some of these molecules are connected with interesting electronic and chemical questions such as conjugation in enediynes, through–space interactions between triple bonds, the position of protonation, charge delocalization in cations, keto–enol (ketene–alkinol, imino–enamine, etc.) tautomerism or Jahn–Teller effects in cumulenes, which consequently are also relevant for enediynes **1**–**13** and, accordingly, will be discussed in this work. Although, it is not the goal of this work to investigate possible rearrangement products of enediynes **1**–**13**, we will discuss in some cases isomers, which are generated by keto–enol tautomerism to clarify the stability of the enediyne structure.

Actually, the present investigation is part of a larger research project, which describes the biochemical activity of enediynes as potential antitumor drugs. Within this project, calculations for more than 200 different molecules have been carried out so that a detailed description of results within one research report is no longer possible. We will describe enediynes, which are more related to the naturally occurring enediynes, the energetics of the Bergman reaction for enediynes **1**–**13** and other enediynes, the properties of the biradicals formed in the Bergman reaction and the biochemical potential of heteroenediynes elsewhere [29].

2. Computational methods

In previous work, we have shown that a reliable geometry of **1** is obtained with Coupled Cluster (CC) employing CCSD(T) theory and a VDZP basis (see Fig. 1, numbers in italics) [16]. B3LYP reproduces the CCSD(T) geometry satisfactorily where the smaller 6-31G(d,p) basis [30] leads to a slightly better agreement with the CC geometry than the larger 6-311 + G(3df,3pd) basis [31] (Fig. 1). Basically,

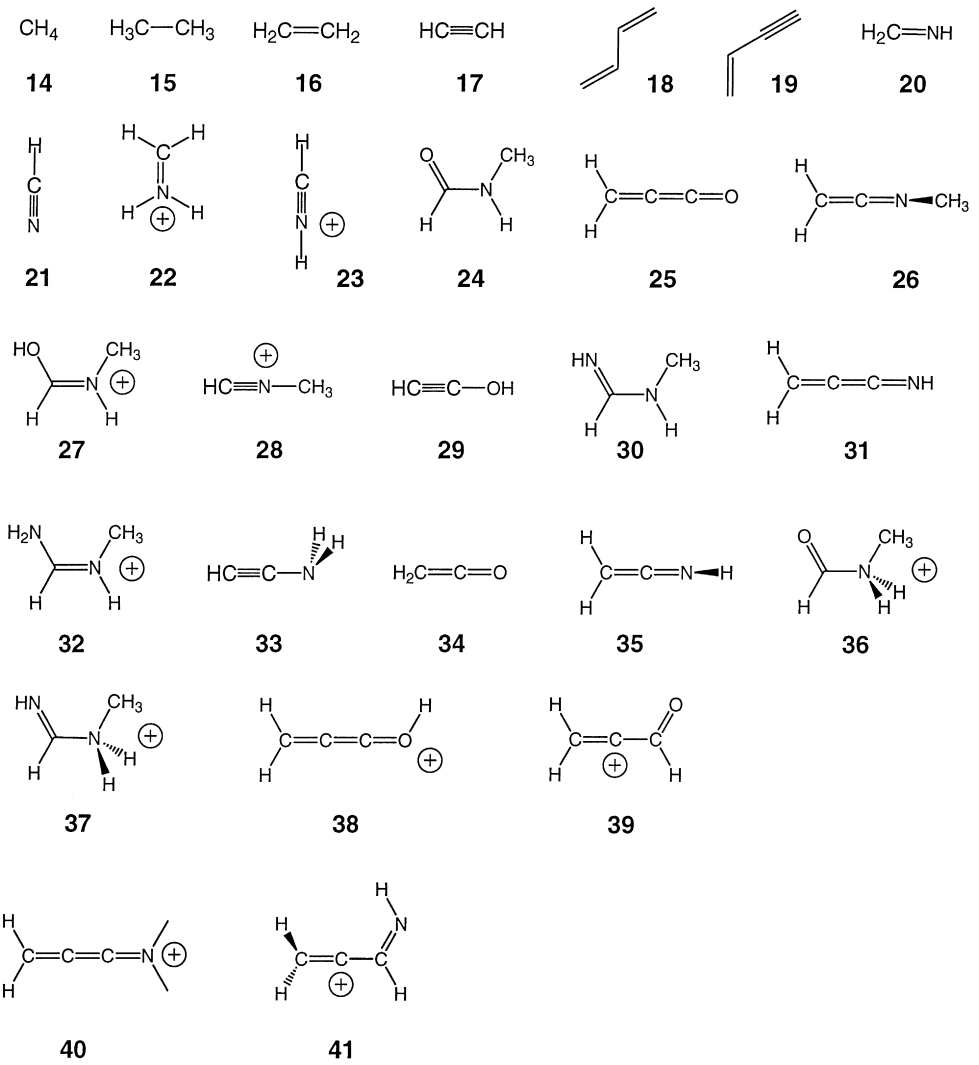

Scheme 3.

DFT makes the formal CC single and triple bonds somewhat too short, which could be interpreted as an exaggeration of bonding and π-delocalization in the 6π system of **1**. However, these differences are small and do not influence the chemical relevance of results obtained at the DFT-B3LYP level of theory. Gräfenstein and co-workers [32] recently demonstrated that hybrid functionals such as the B3LYP functional of Becke [33–36] provide the best DFT description of the Bergman cyclization of **1** and as the present work is part of a larger research project including many molecules related to the enediyne chemistry, we have chosen B3LYP/6-31G(d,p) as both an economic and reliable alternative to CCSD(T) to investigate enediynes **2**–**13** as well as the reference molecules **14**–**41** listed in Scheme 3.

For the DFT calculations, the standard pruned (50,194) fine grid [37] was used, which is a reasonable compromise between calculational time and accuracy. For each molecule investigated, geometry and vibrational frequencies were calculated. The latter were used to verify local/global minimum character of the stationary points found in the geometry calculations and to calculate zero-point energies (ZPE). Some of

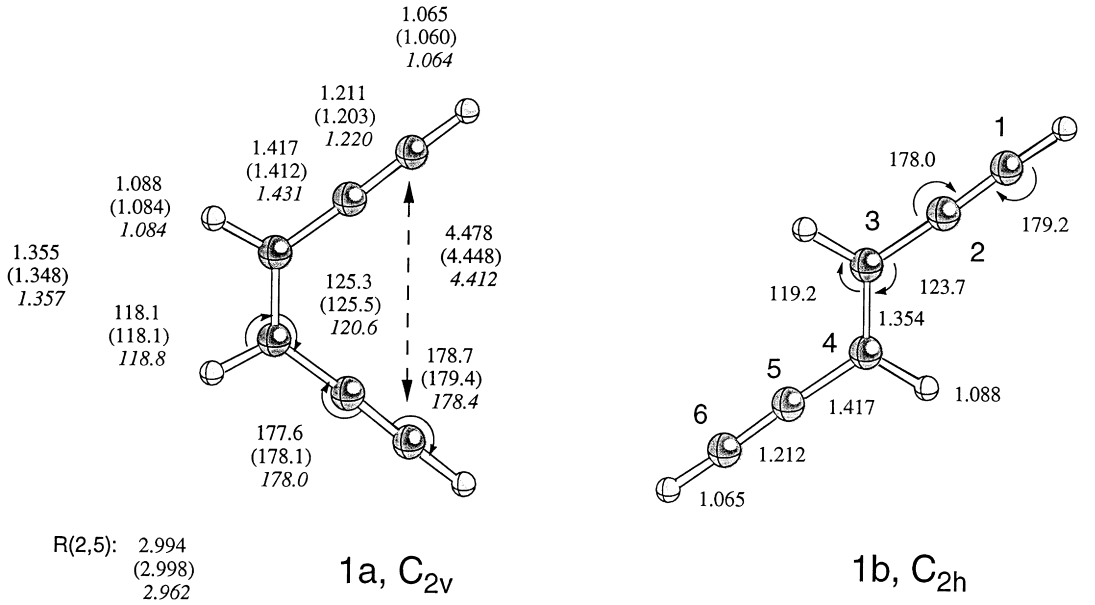

Fig. 1. B3LYP/6-31G(d,p) geometry of (*Z*)-hex-3-ene-1,5-diyne (**1a**) and (*E*)-hex-3-ene-1,5-diyne (**1b**). For **1a**, results obtained at the B3LYP/6-311 + G (3df3pd) (in parentheses) and at the CCSD(T)/6-31G(d,p) level of theory (in italics) are also given. Lengths in Å and angles in degree.

the molecules investigated turned out to be conformationally very flexible due to internal rotations and bent–linear–bent inversions. By analysis of the low-frequency modes and additional calculations, it was verified that the most stable conformation had been found. Enthalpies at 298 K were also calculated, however since we analyze in the present work just electronic differences between the enediynes they

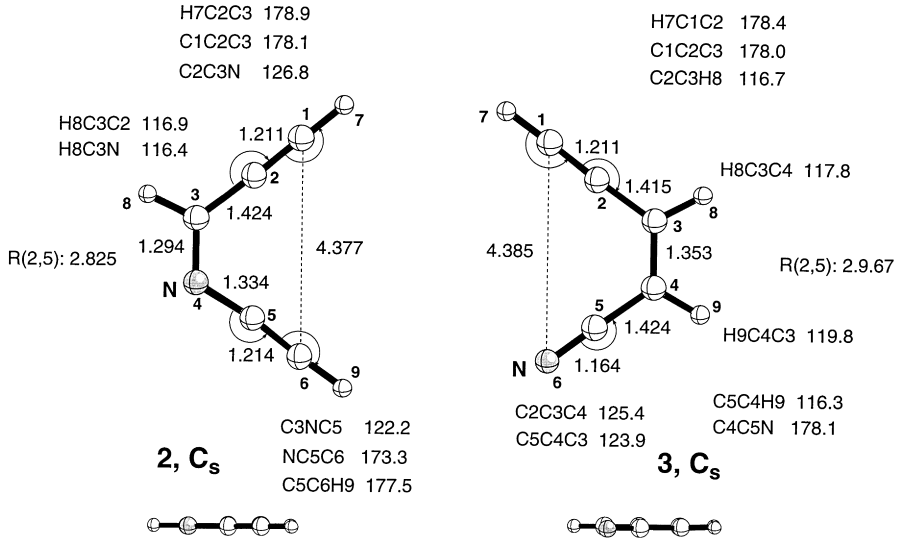

Fig. 2. B3LYP/6-31G(d,p) geometry of (*Z*)-3-aza-hex-3-ene-1,5-diyne **2** and (*Z*)-pent-3-ene-1-yne-nitrile **3**. Lengths in Å and angles in degree.

Table 1
Absolute energies, zero point energies ZPE, frequencies ω_{low} and dipole moments μ for enediynes 1–13 and reference molecules **14–41** calculated at B3LYP/6-31G(d,p) (energies in hatree, zero point energies in kcal/mol, frequencies in cm^{-1}, and dipole moments in Debye. Dipole moments of charged molecules are given with regard to a coordinate system based on the center of charge. ω_{low} denotes the lowest harmonic frequency calculated where only values $<300\ cm^{-1}$ are given. The magnitude of ω_{low} indicates the conformational flexibility of the molecule in question and verifies the minimum nature of the stationary point)

Molecule	Energy	ZPE	ω_{low}	μ
1a	−230.88718	44.4	108	0.09
1b	−230.88838	44.2	124	0
2	−246.91554	36.8	108	2.32
3	−246.98165	37.9	107	3.74
4	−247.26161	45.6	110	1.23
5	−247.30715	44.5	103	3.20
6	−361.47433	57.6	77	2.53
7a	−361.51204	58.6	52	5.26
7b	−361.51399	58.6	66	2.83
8	−361.82014	65.9	22	1.90
9a	−361.86641	66.3	3	1.32
9b	−361.92013	66.4	14	4.30
9c	−361.90878	66.4	58	5.08
10	−361.59097	65.3	46	1.19
11a	−341.62659	65.7	45	2.90
11b	−341.68001	66.4	67	6.52
11c	−341.68376	66.5	69	4.62
12	−341.97347	73.8	73	2.85
13a	−342.02732	74.0	20	2.58
13b	−361.04442	73.4	22	2.12
13c	−361.03322	73.5	67	0.85
14	−40.52401	28.2		0
15	−79.83874	47.0		0
16	−78.59381	32.1		0
17	−77.32957	35.2		0
18	−156.00166	53.5	176	0
19	−154.74043	38.3	228	0.34
20	−94.63345	25.1		1.95
21	−93.42458	10.3		2.89
22	−94.98363	34.1		0.43
23	−93.70886	17.5		0.34
24	−209.20926	46.7	76	3.80
25	−190.65907	23.4	139	2.49
26	−172.03061	45.5	143	1.47
27	−209.55663	55.5	71	2.70
28	−133.05493	35.6		1.77
29	−152.53905	19.8		1.79
30	−189.32191	54.4	125	2.58
31	−170.78068	30.8	193	1.97
32	−189.71558	63.4	116	1.39
33	−132.68695	27.7		1.86
34	−152.60202	19.9		1.49
35	−132.71834	27.5		1.59

Table 1 (*continued*)

Molecule	Energy	ZPE	ω_{low}	μ
1a	−230.88718	44.4	108	0.09
36	−209.52695	54.9	97	4.88
37	−189.66412	63.2	109	3.46
38	−190.94908	31.0	222	1.88
39	−190.90726	28.1	175	5.76
40	−171.13282	39.3	226	1.42
41	−171.06125	38.0	98	3.53

are published elsewhere [29]. Charge distributions were investigated by employing the natural atomic orbital (NAO) population analysis [38–40]. All calculations were performed with the ab initio programs COLOGNE 99 [41] and GAUSSIAN 98 [42].

3. Results and discussions

Calculated energies of molecules **1**–**41** are listed in Table 1. Table 2 summarizes the proton affinities (PA) relevant for the discussion of the stability of protonated enediynes. In Figs. 2–7, calculated geometries of enediynes **2**–**13** ordered in pairs of isomers are shown while Fig. 8 contains the most important geometrical parameters of reference molecules **18**–**41**. Formal reactions shown in Schemes 4–10 are used to elucidate the stability of the various enediynes. Scheme 11 gives keto–enol-type arrangements for some reference molecules, which are needed to predict the most stable form of enediynes **7**, **9**, **11**, and **13** (see Scheme 12).

All enediynes investigated, but **7** and **11** are essentially planar in the enediyne part since the largest out-of-plane deviations are lower than 1°. Although the geometry optimization was performed without any symmetry constraint, C_s symmetry is fulfilled within computational accuracy for all enediynes investigated with the exception of **7** and **11**, which will be discussed in more detail in the following. It is interesting to note that theory predicts regular deviations from a linear arrangement for the ethinyl parts. This was observed before [16], however not discussed, as the deviations seemed to be too small to be of any significance. As shown in Figs. 1–7, there is a regular pattern of deviations, which can lead to CCC and CCH angles differing by up to 8° from the 180° angles

Table 2
Proton Affinities PA of Hetero-endiynes and some reference molecules calculated at B3LYP/6-31G(d,p) (proton affinities and ΔE values in kcal/mol. ΔE gives the in(de)crease of the PA as E(ref)−E(mol) so that negative values indicate stabilization of the molecule in question upon protonation relative to the protonated reference molecule)

A + H^+ → HA^+	Side of protonation	PA	Ref. molecule	ΔE
2 → 4	=N–	217.2	**20**	2.5
3 → 5	≡N	204.2	**21**	−25.8
6 → 8	=O	217.0	**24**	1.0
7 → 9	=O	222.4	**25**	−35.0
10 → 12	=NH	240.0	**6**	−23.0
			30	7.0
11 → 13	=NH	251.5	**7**	−29.1
20 → 22	=NH	219.7		
21 → 23	≡N	178.4	**20**	41.3
24 → 27	=O	218.0		
24 → 36	–NHMe	199.3	**20**	20.4
25 → 38	=O	182.0	**31**	−30.4
25 → 38	=C=	155.7		
30 → 32	=NH	247.0	**24**	−29.0
30 → 37	–NHMe	214.7	**24**	−15.4
31 → 40	=NH	221.1	**25**	−39.9
31 → 41	=C=	176.1	**25**	5.9

of the linear arrangement. Deviations result from through–space interactions between the triple bonds, which are largest between the in-plane π-orbitals and are of the 4-electron repulsive nature thus widening angles of C2C3C4 and C3C4C5 (or the corresponding angles for the N-containing enediynes, see Fig. 9(a) and (b)). This is confirmed by the calculated values of these angles (e.g. 125.3° for **1a**, Fig. 1) although DFT

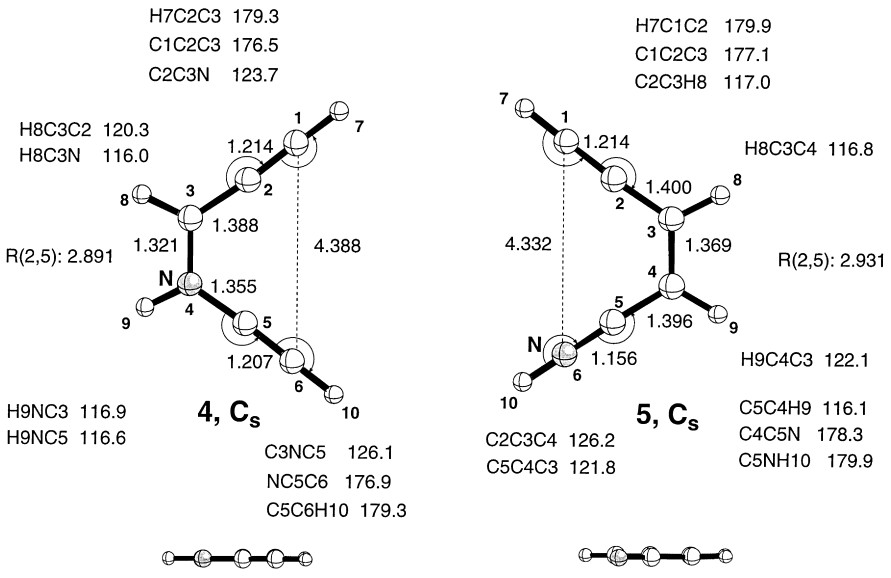

Fig. 3. B3LYP/6-31G(d,p) geometry of N-protonated (*Z*)-3-aza-hex-3-ene-1,5-diyne **4** and N-protonated (*Z*)-pent-3-ene-1-yne-nitrile **5**. Lengths in Å and angles in degree.

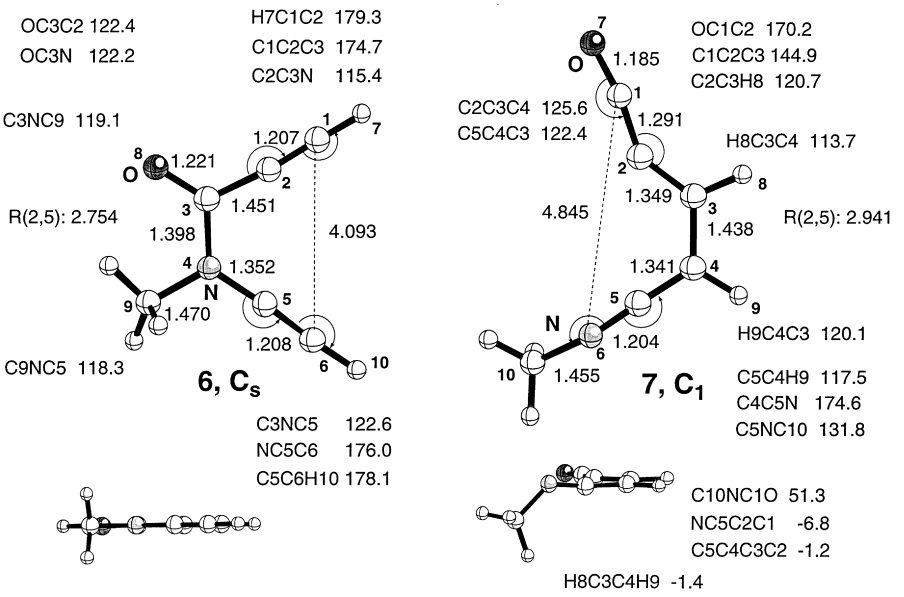

Fig. 4. B3LYP/6-31G(d,p) geometry of amide **6** and oxocumulene (**7**). Lengths in Å and angles in degree.

might slightly exaggerate angle widening because of the shorter C2C3 and C4C5 bond lengths as compared to the corresponding CCSD(T) values (Fig. 1). An outward bending of the C1C2C3 and C4C5C6 units leads to an additional lowering of through−space repulsion between the triple bonds as is schematically indicated in Fig. 9(b) (direction 3).

The inward bending of the terminal CH bonds is a

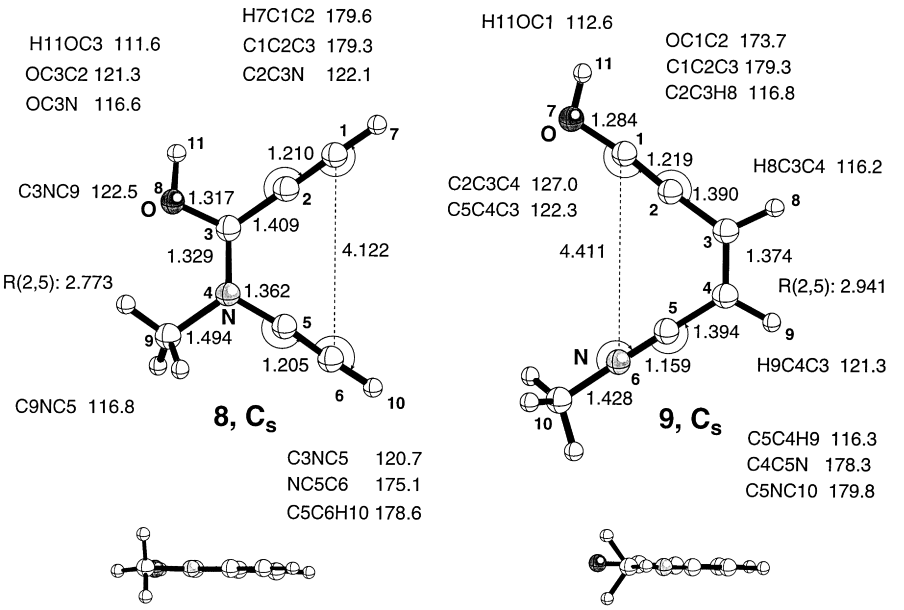

Fig. 5. B3LYP/6-31G(d,p) geometry of O-protonated amide **8** and O-protonated oxocumulene (**9**). Lengths in Å and angles in degree.

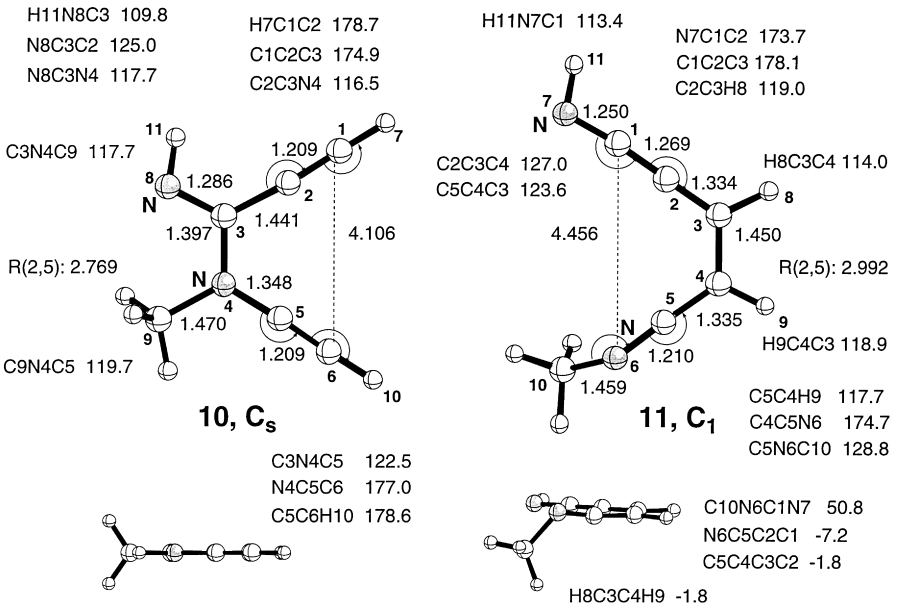

Fig. 6. B3LYP/6-31G(d,p) geometry of amidine **10** and azacumulene (**11**). Lengths in Å and angles in degree.

necessary consequence of the small rehybridization at C2 and C5 and thus increases the overlap for in-plane π bonding of the triple bonds (Fig. 9(b)). Through bond interactions between the triple bonds, which would involve the σ^*(C3C4) orbital and which would require collinearity between the corresponding orbitals, does not seem to play any role as it would enforce the opposite bending modes of the ethinyl

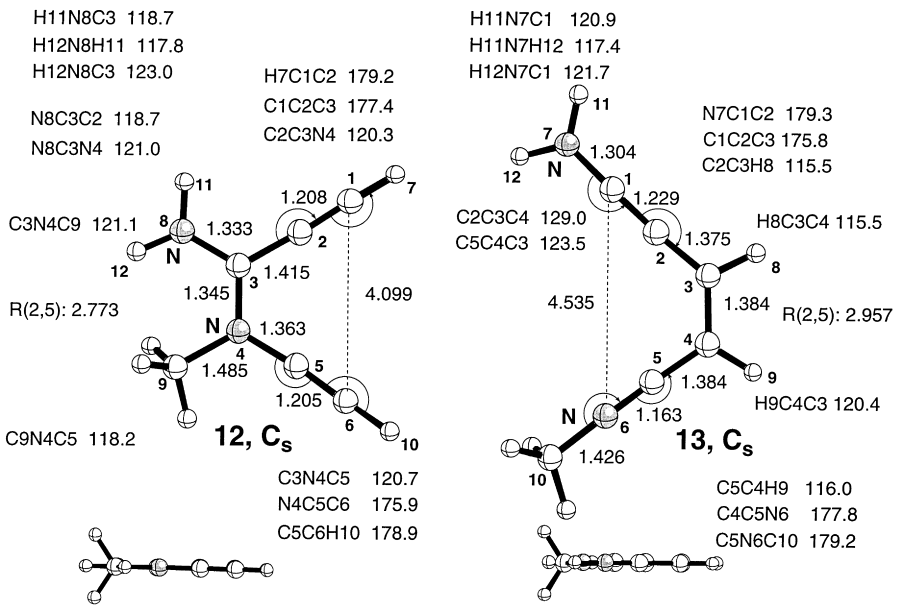

Fig. 7. B3LYP/6-31G(d,p) geometry of protonated amidine **12** and protonated azacumulene (**13**). Lengths in Å and angles in degree.

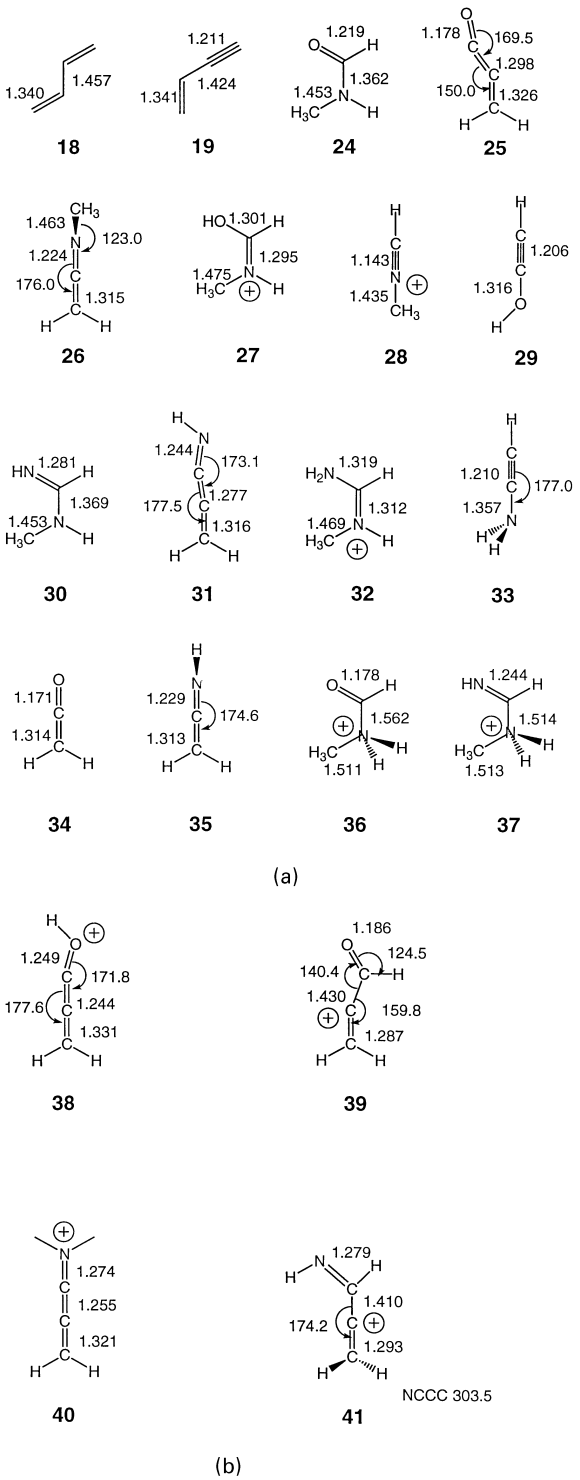

Fig. 8. B3LYP/6-31G(d,p) geometries of reference molecules. Lengths in Å and angles in degree.

Table 3
Bond lengths (in Å) of reference molecules (position of the bond refers to the position of the bond type in enediynes **1**–**13** (see Scheme 1). Reference molecules are listed in Scheme 3)

Position of bond	Type of bond	Ref. molecule	Value
1	–C≡C–	*HC≡CH*	1.206
1	=C=C=	**31**	1.277
		25	1.298
2	⟩C=C=	**31**	1.316
		25	1.326
3	⟩C=C⟨	**28**	1.340
		(*H_2C=CH_2*)	(1.330)
2	=C–C≡	**19**	1.424
4	=C–C=	**18**	1.457
5	–C≡N^+–	**28**	1.143
1	–C≡N–	*HC≡N*	1.157
1	=C=N–	**31**	1.244
3	–C=N–	*H_2C=NH*	1.270
3	–C=N^+⟨	*H_2C=NH_2^+*	1.278
3	–C=N⟨	**24**	1.362
		30	1.369
2	≡C–N⟨	**33**	1.357

substituents. The non-linearity of the ethinyl units influences distances $R(1,6)$ and $R(2,5)$ given in Figs. 1–7. In previous work, a relationship between these geometrical parameters and the energy barrier of the Bergman reaction was established for derivatives of **1** [16,43], however, in the present study such a relationship could not be confirmed, obviously because of the different electronic structures of the enediynes investigated.

Table 4
Bond equilibration in enediynes **1**–**13**. Changes in bond lengths relative to those of the reference molecules of Table 3 are given in 10^{-3} Å (the position of the bond follows the numbering of atoms shown in Scheme 1)

Molecule	Bond 1	Bond 2	Bond 3	Bond 4	Bond 5
1	5	− 7	15	− 7	5
2	5	0	24	− 23	8
3	5	− 9	13	0	7
4	8	− 36	43	− 2	1
5	8	− 24	29	− 28	13
9	13	− 34	34	− 30	16
13	23	− 49	44	− 40	20
6	1	27	26	− 5	2
10	3	17	28	− 9	3
8	4	− 15	34	5	− 1
12	2	− 9	33	6	− 1
7	− 7	23	− 19	25	− 40
11	− 8	18	− 7	19	− 34

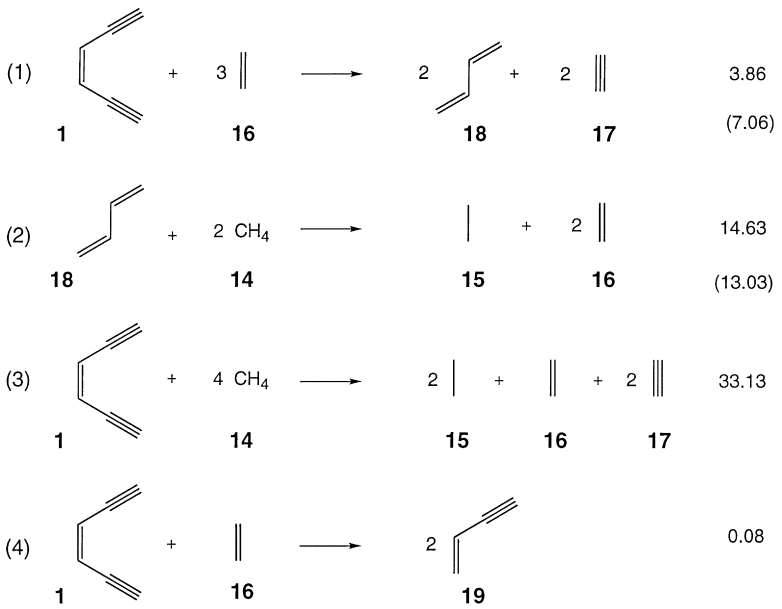

Scheme 4.

Compared to the typical bond lengths of the reference molecules listed in Table 3, there is a regular pattern of bond equilibration in most of the enediynes as indicated in Table 4 and Fig. 9(c): Multiple bonds become longer and formal single bonds shorter, which is particularly clear if the acetylene bond length is used as a reference. However, in general, calculated changes in bond lengths are rather small suggesting

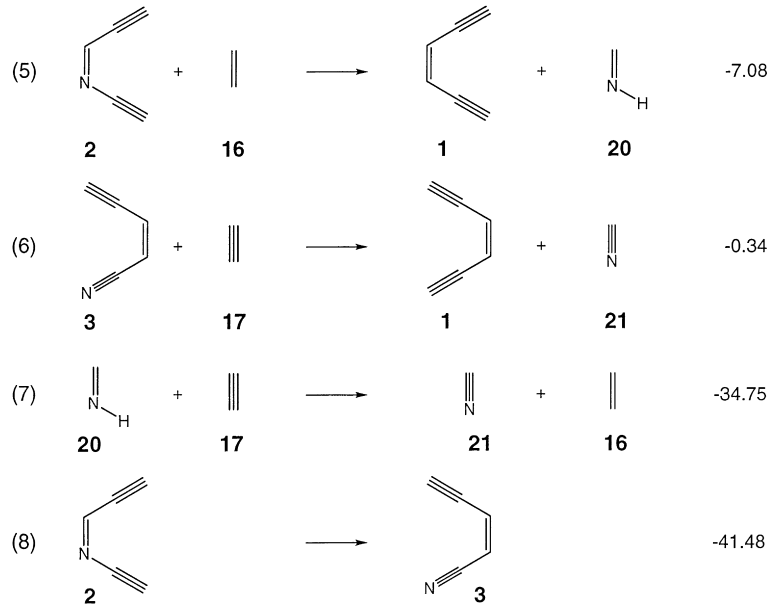

Scheme 5.

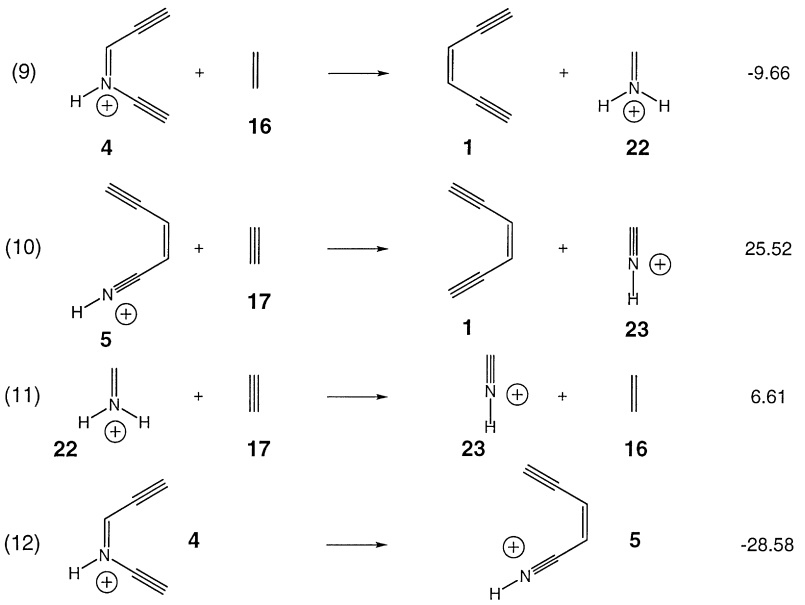

Scheme 6.

that π-delocalization is similar to that in polyenes. For example, if the triple bond of vinylacetylene **19** is used as reference bond, changes of the triple bonds will be much smaller indicating that, e.g. π-delocalization in **1** is similar to that in **19**, which means that the incorporation of the second ethinyl substituent does not increase π-stabilization very much. In the case of cross conjugation as in the amide **6** or the

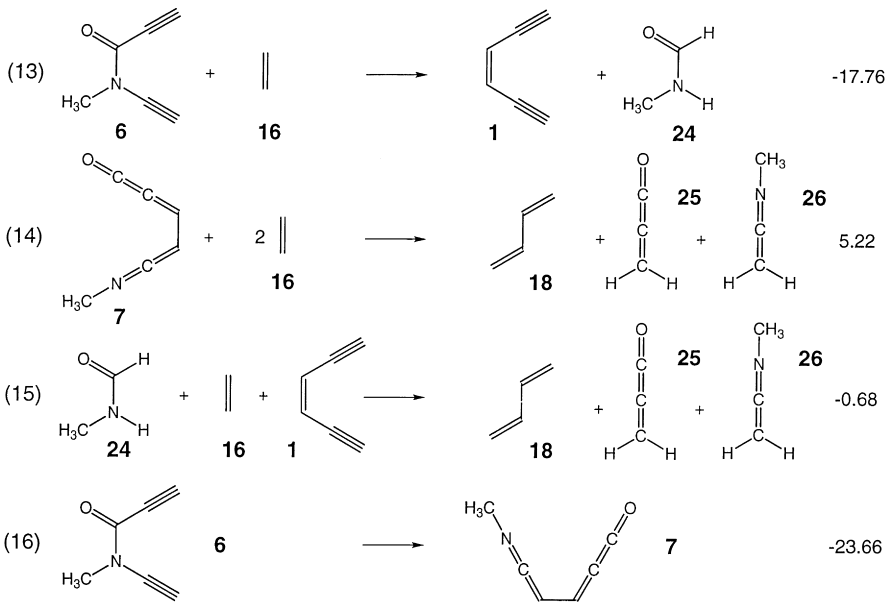

Scheme 7.

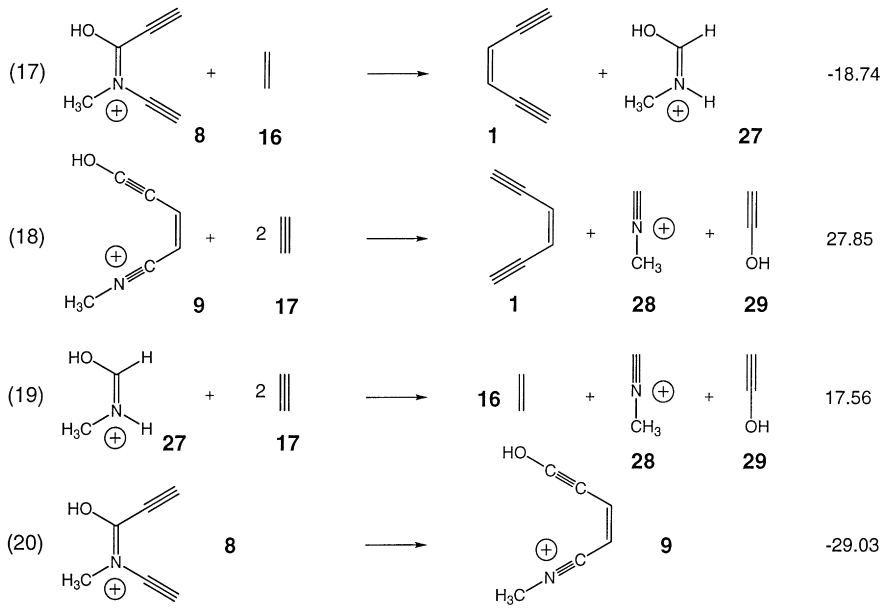

Scheme 8.

amidine **10**, the bond equilibration pattern is disturbed (Table 4). This is also true for the corresponding protonated molecules where in these cases, a positive N atom in position 4 seems to represent a strong perturbation (see also **4**, Table 4). Cumulenes **7** and **11** have a different bond equilibration pattern (Fig. 9(d)), which can be interpreted to lend the molecule some enediyne character. However, changes are too

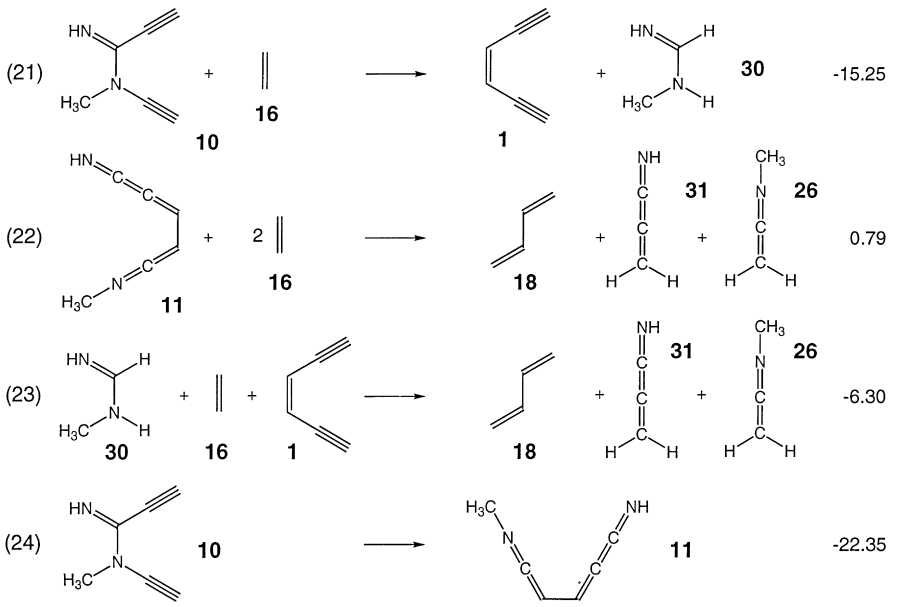

Scheme 9.

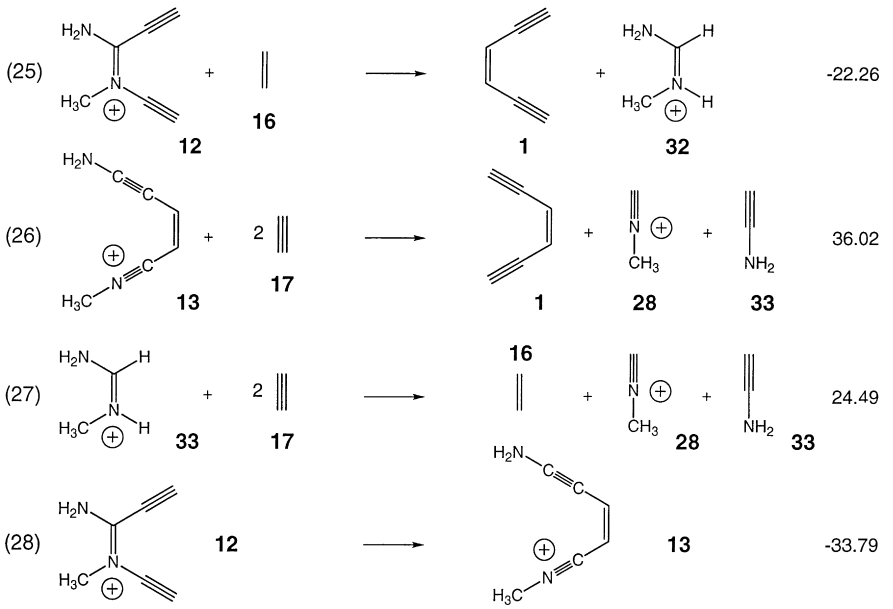

Scheme 10.

small to speak of zwitterionic (enediyne) character in these cases.

3.1. Structure and stability of (Z)-hex-1,5-diyne-3-ene (1)

The stability of **1a** is assessed by formal reactions (1)–(4) of Scheme 4. π-Delocalization in **1** is slightly higher relative to *trans* 1,3-butadiene **18** as an appropriated reference for conjugation, because 6 rather than 4π electrons are delocalized (reaction 1). The bond separation energy of *trans* **18** (see reaction 2) is 14.6 kcal/mol; half of which is due to π-delocalization while the other half results from the changes in

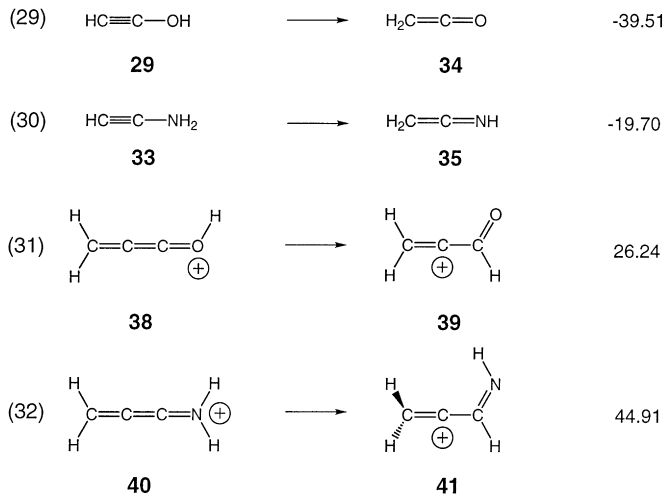

Scheme 11.

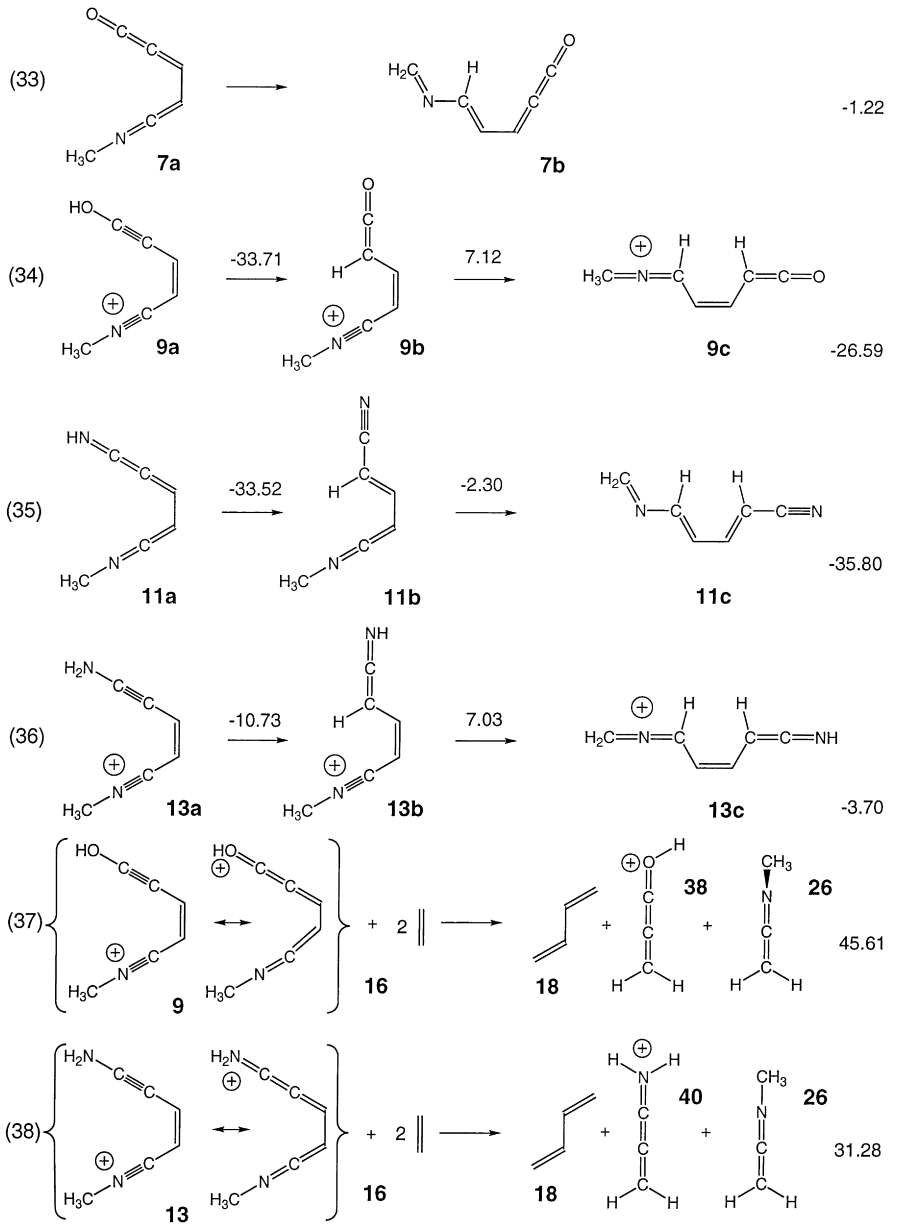

Scheme 12.

bond lengths if standard single and double bonds are incorporated in a conjugated system [44]. Since *cis* 1,3-butadiene (*cis*-**18**), which may be considered as a more appropriate reference, is less stabilized by π-delocalization (lowering by 1.6 kcal/mol; steric effects add another 1.4 kcal/mol leading to a destabilization by about 3 kcal/mol [44]), a reasonable estimate for the stabilization energy of **1** due to π-delocalization is $7.1 + 2(7.3 - 1.6) = 18.5$ kcal/mol. (In Scheme 4, numbers in parentheses refer to changes in the π-delocalization energy using *cis* 1,3-butadiene as reference.) Considering addition changes in bond

lengths, the total bond separation energy of **1** (see reaction 3) is 33.1 kcal/mol. In line with the relatively little degree of bond equilibration discussed above, there are no significant interactions between the triple bonds that becomes obvious when considering reaction 4, which is endothermic by just 0.1 kcal/mol.

The heat of formation of **1a** was estimated to be 126.4 (CCSD(T) calculations [16]) and 124.4 kcal/mol (thermochemical group increments [45]). A value of 119.8 is obtained by using the B3LYP reaction enthalpy at 298 K (3.69 kcal/mol) form the formal reaction (1), which indicates that B3LYP exaggerates somewhat the stability and, in particular, the π-delocalization of **1** in line with the observation that the calculated CC single and triple bonds are somewhat too small. Since the B3LYP energy (and enthalpy) difference between *Z* and *E* forms of **1** is 0.8 kcal/mol (Table 1) in agreement with an estimated value of 0.6 kcal/mol in favor of the *E* form [45], the overestimation of π-delocalization seems to apply to enediynes independent of their configuration.

(*Z*)-3-aza-hex-3-ene-1,5-diyne **2** and the isomeric nitrile **3**. When a N atom is incorporated into enediyne **1** at position 3, π-delocalization is perturbed (see also Table 4) and the stability of the aza-enediyne formed is lower than that of the parent compound. According to reaction (5) (see Scheme 5), which compares enediynes **2** and **1**, the π-stabilization energy of the former molecule is 7.1 kcal/mol smaller than that of the latter molecule. Incorporation of the N atom at position 1 thus leading to nitrile **3** has little effect on the π-delocalization as is indicated by the B3LYP reaction energy of reaction (6) (−0.3 kcal/mol, Scheme 5). In line with this result is the fact that the geometry of **3** is similar to that of **1** (see Figs. 1 and 2). Reactions (5) and (6) do not provide any information on the relative stability of enediynes **2** and **3** as they are based on a comparison of double (reaction 5) and triple bonds (reaction 6) with and without N. The B3LYP energy of *normalization* reaction (7) reveals that the C≡N bond is almost 35 kcal/mol more stable in relation to the C≡C triple bond than the C=N double bond in relation to the C=C double bond. Hence, nitrile **3** is 41.5 kcal/mol more stable than the aza-enediyne **2** because of the transfer of the N atom from the unfavorable position 3 to the more favorable position 1 (35 kcal/mol) and the increase in π-delocalization (7 kcal/mol, Scheme 5). This energy difference should represent a thermodynamic force to rearrange **2** via Bergman reaction and subsequent retro-Bergman reaction involving the CN bond to yield the much more stable isomer **3** (see Scheme 1).

*3.2. Protonated enediynes **4** and **5***

The PA of **2** is 217 and that of **3** just 204 kcal/mol (Table 2) while the corresponding B3LYP values for the reference molecules formaldimine (**20**) and HCN (**21**) are 219.7 and 178.4 kcal/mol, respectively. Protonation of a nitrile is less favorable than that of an aldimine where the large difference in PA values (41.3 kcal/mol, Table 2) can be lowered to 13 kcal/mol if the positive charge is better delocalized in the more extended π system of an enediyne. These considerations are important to understand the relative stability of protonated enediynes **4** and **5**.

The B3LYP energy of formal reaction (9) of Scheme 6 suggests that stabilization resulting from π-delocalization is 10 kcal/mol lower in **4** than in **1**. A comparison of **5** with the parent enediyne **1** according to reaction (10) of Scheme 6 leads to a stability difference of 25.5 kcal/mol in favor of the former molecule. However, this is mainly as a result of constraining the more favorable charge delocalization in **5** to the CN triple bond of **23**, which causes a change in the calculated PA values by 28 kcal/mol.

Enediyne **5** with N in the terminal position is still more stable than enediyne **4** with N in the central position, however protonation reduces the stability difference from 41.5 to 28.6 kcal/mol. Also, the reason for the stability difference is no longer the difference in the bond strengths of C=N and C≡N bond in relation to that of the corresponding CC bonds (this difference is changed from −34.7 to 6.6 kcal/mol according to Scheme 6, reaction 11), but mainly the favorable charge delocalization in **5**.

*3.3. Amide **6** and the isomeric oxocumulene **7***

Amide **6** is the parent molecule of a possible class of molecules that were suggested by Chen and coworkers [19] as a basis for new enediyne antitumor drugs replacing simple aza-endiynes such as **2**, which have several disadvantages. In a parallel work, we have suggested that amidines may be actually better suited as potential drugs [29]. Therefore, both amides

and amidines as well as their protonated counterparts were the primary target of this investigation.

Amides are known to possess a CN bond with partial double bond character [46], which is reflected by a CN bond length of 1.362 Å calculated for amide **24** (Fig. 8). In **6**, the CN bond is elongated to 1.398 Å (Fig. 4) indicating that π-delocalization in the amide system is disturbed by the ethinyl substituents. The analysis of bond equilibration in **6** (Table 4) reveals that the stability of the amide suffers from cross-conjugation, which is confirmed by a value of −17.8 kcal/mol for the energy of reaction (13) of Scheme 7, which compares **6** with **1**. Neither dipole moment (2.5 Debye, for **24** the dipole moment is 3.8 Debye, Table 1), geometry (Fig. 4, Table 4) nor calculated NAO charges indicate in any way that amide **6** has some zwitterionic (enediyne) character as proposed in Scheme 2. The cumulene **7** is more stable by 23.7 kcal/mol than the isomeric amide **6** (Scheme 7, reaction 16). This is almost exclusive due to the different π-stabilization energies of the two isomers (comparison of reactions 13, 14, and 15 in Scheme 7).

Cumulene **7** contains an oxocumulene and an azaallene unit connected by a formal CC single bond in the same way as the two double bonds in *cis* 1,3-butadiene. This connection increases the π-delocalization energy of **7** by 5.2 kcal/mol relative to *trans*- and by 6.8 kcal/mol relative to *cis* 1,3-butadiene (see Scheme 7 and 4). The energy of reaction (15), which provides the balance between reactions (13) and (14) with regard to the reference compounds used in these reactions, is negligible and, therefore, the larger stability of **7** is primarily due to the destabilization of amide **6** by cross-conjugation.

It is interesting to note that neither the oxocumulene unit (OCC = 170.2, CCC = 144.9°) nor the azaallene unit (NCC = 174.6°) of **7** are linear (Fig. 4). This is also the case for reference molecules **25** (OCC = 169.5, CCC = 150.0°) and **26** (NCC = 176.0°, see also **35** in Fig. 8). In connection with the well-known non-linearity of cumulenes [47], the possibility of a second-order Jahn–Teller effect was discussed [48].

*3.4. Protonated enediynes **8** and **9***

Amides are known to be protonated at the O atom, however, exceptions are also known [49]. In the present case, we compared O- and N-protonation for reference amide **24**. As reflected by the PA values of Table 2, O-protonation is more favorable than N-protonation by 19 kcal/mol. Also, protonation at O establishes formally the enediyne structure in amide **6** (and cumulene **7**; see Fig. 5 and Table 4) while protonation at the N atom destroys π-delocalization in the amide part and by this also in the enediyne. Therefore, the possibility of N-protonation can be excluded for amide **6**.

Despite the formal enediyne character of **8**, its stability is slightly lower than that of **6** as reflected by the energy of reaction (17) in Scheme 8 (−18.7 kcal/mol) and the difference of the energies for reactions (13) (Scheme 7) and (17) (1.0 kcal/mol). This is a result of: (a) perturbation by a positively charged N atom, and (b) the destabilizing influence of the π-donor/σ-attractor OH.

Reaction (10) of Scheme 6 and reaction (18) of Scheme 8 are related as is reflected by the calculated reaction energies of 25.5 and 27.8 kcal/mol. In both cases, the endothermicity of the reaction is caused by decreasing the possibility of charge delocalization. Therefore, it is understandable that the nitrilium cation **9** is more stable by 29 kcal/mol than the isomeric iminium cation **8** similar to the stability difference between **4** and **5** (28.6 kcal/mol, Scheme 6).

Enediyne **9** possesses an ethinol rest, which should easily rearrange to a ketene. For the reference system **29** → **34**, B3LYP predicts a large energy gain of 39.5 kcal/mol (Scheme 11). Therefore, it was appropriate to calculate beside **9a** its ketene isomers **9b** and **9c** (see Scheme 12 and Fig. 10), where the latter molecule is formed by H migration from the terminal methyl group to the C atom at position 6. Both **9b** and **9c** are more stable than **9a** by 33.7 and 26.6 kcal/mol, respectively. Since the barrier for a alkinol–ketene rearrangement should be relatively small, it is unlikely that enediyne **9a** can be synthesized or captured as an intermediate product of the two-step reaction from **8** to **9** (compare with the reaction in Scheme 1).

The question whether **9a** possesses any character of a protonated ketene has to be denied in view of its bonding pattern and the large endothermicity (45.6 kcal/mol) of decomposition reaction (37) in Scheme 12. Actually, oxocumulenes are protonated at

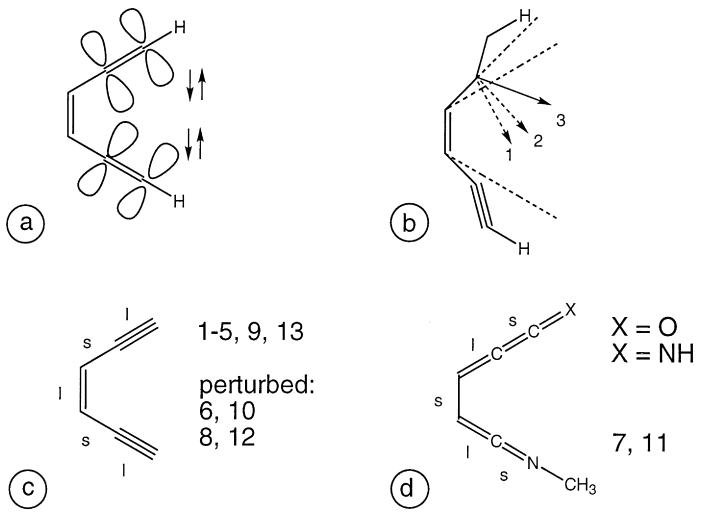

Fig. 9. Distortions of the enediyne geometry. (**a**) Through-space interactions between the in-plane π-orbitals of the triple bonds in (*Z*)-hex-3-ene-1,5-diyne (**1a**). (**b**) Schematic drawing of the distortion of the linear ethinyl substitutents. Arrows 1 and 2 give the directions of the in-plane π-orbitals of the triple bonds before (direction 1) and after the widening of the angle ≡C–C=C (direction 2). Direction 3 results from the outward bending of C–C≡C. (**c**) Bond equilibration pattern of normal enediynes **1**–**5**, **9**, and **13**. (**d**) Bond equilibration pattern for heterocumulenes **7** and **11**. Abbreviations *l* and *s* denote lengthening and shortening of bonds in relation to bonds in appropriate reference molecules shown in Table 3 (compare also with Table 4).

the O atom and not at one of its CC double bonds. As reaction (31) of Scheme 11 reveals the vinyl cations formed are strongly destabilized (26.2 kcal/mol) by the formyl rest. Similar conclusions can be drawn for azacumulenes such as **31**, which are also preferentially protonated at the NH group. Molecule **40** is 45 kcal/mol more stable than the corresponding vinyl cation **41** (see reaction 32 of Scheme 11).

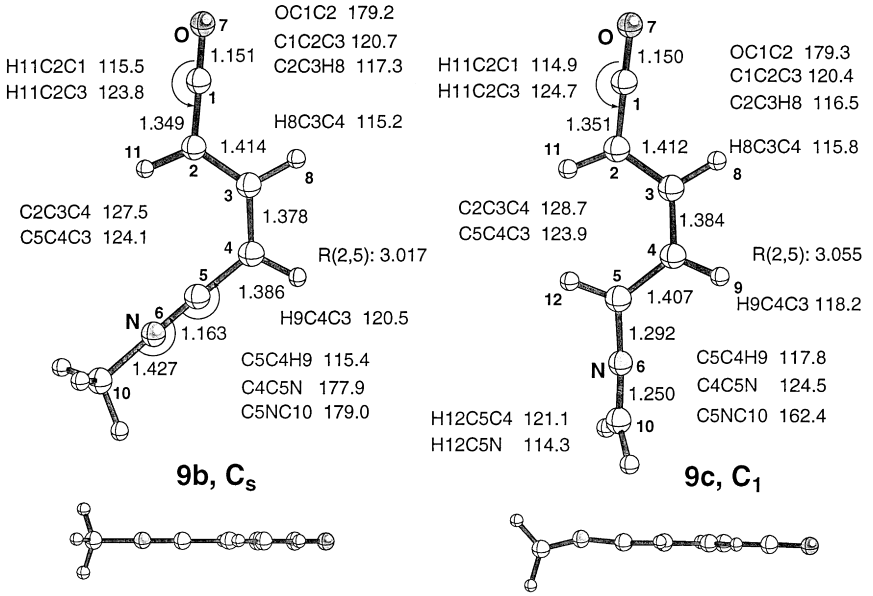

Fig. 10. B3LYP/6-31G(d,p) geometry of isomers **9b** and **9c** of protonated oxocumulene (**9a**). Lengths in Å and angles in degree.

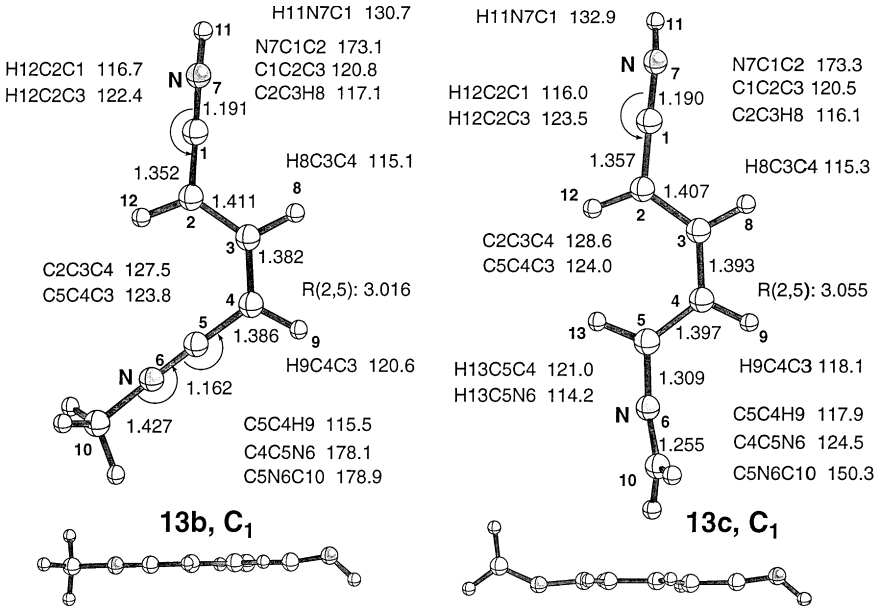

Fig. 11. B3LYP/6-31G(d,p) geometry of isomers **13b** and **13c** of protonated azacumulene (**13a**). Lengths in Å and angles in degree.

*3.5. Amidine **10** and its isomer **11***

Amidine **10** should posses similar properties as amide **6**, which is confirmed by its geometry (Fig. 6, Table 4) and the reaction energies summarized in Scheme 9. Cross-conjugation is less problematic (increase of bond length 2 is 0.017 Å rather than 0.027 Å as for **6**, Table 4, Fig. 6) and, therefore, **10** is destabilized relative to **1** by just 15.2 kcal/mol (see reaction (21) in Scheme 9) rather than 17.8 kcal/mol as in the case of the amide **6**. Similarly, π-delocalization in the azacumulene **11** is 4.4 kcal/mol smaller than in the oxocumulene **7** (energy of reaction (22): 0.8 kcal/mol, Scheme 9). As in the case of the amide, amidine **10** is more than 20 kcal/mol (22.4; **6**: 23.7, Schemes 9 and 7) less stable than the cumulene **11**, which again is primarily due to the loss of π-delocalization energy in the amidine because of cross-conjugation. Calculated NAO charges and dipole moments of **10** and reference molecule **30** (Table 1) do not indicate any participation of the zwitterionic (enediyne) resonance structure shown in Scheme 2.

The heavy atom framework of azacumulene **31** is non-linear where the bending angles are somewhat smaller (NCC 173.1; CCC = 177.5°, Fig. 8) than for the oxocumulene **25**. The same is true for the azacumulene unit of **11** (NCC 173.7; CCC = 178.1°, see Fig. 6). Aza-allenes such as **35** or **26** are also slightly bend (NCC 174.6; 176.0°, Fig. 8). Since the substituent at N is located perpendicular to the CH_2 plane, the bending leads to a slight *trans* arrangement of N-substituent and the C atom of the CH_2 group. The aza-allene structure of **11** bears the same structural features (NCC 174.7°, CNC5C4 = 178°, Fig. 6), which causes some non-planarity for the heavy-atom framework C1C2C3C4C5N of **11** as shown in Fig. 6. Calculations show that **11a** is actually less stable than the nitrile **11b** by 33.5 kcal/mol (Scheme 12), which is easily formed by H migration. Isomer **11c**, however, is unlikely to be formed. We conclude that **11a** similar to **7a** will be difficult to synthesize and to capture.

*3.6. Protonated enediynes **12** and **13***

The PA values of amidine **10** and azacumulene **11** are 240 and 251 kcal/mol, respectively (Table 2), which have to be compared with the PA values of the corresponding reference molecules **30** and **31** (247; 221 kcal/mol, Table 2). Protonation of amidine **30** at the amine-N atom (215 kcal/mol, Table 2) is 32 kcal/mol less exothermic than protonation at the =NH group and, therefore, can be excluded similarly

as in the case of the amide. The PA values of **6** and **10** clearly show that the amidine is much more basic (PA is larger by 23 kcal/mol, Table 2) than that of the corresponding amide. This is confirmed by the known pK_A values of amidines typical of strong organic bases [50,51] and should guarantee protonation in the weakly acidic medium of a tumor cell.

Although protonation formally establishes the enediyne structure for amidine **10**, it disturbs π-delocalization stronger (loss of 7 kcal/mol π-stabilization energy) than in the case of the amide as is reflected by an energy of −22.3 kcal/mol for reaction (25) of Scheme 10 (compared to −15.3 kcal/mol for the neutral molecule, reaction 21, Scheme 9).

Since the protonated azacumulene **13** can delocalize its positive charge in the enediyne system, the neutral molecule **11** has also a high PA value, which is 30 kcal/mol larger than that of reference **31** (Table 2). The magnitude of stabilization is also reflected by the energy of formal reaction (26) of Scheme 10 (36 kcal/mol) and the calculated energy difference of 33.8 kcal/mol between isomers **12** and **13**. The tautomeric rearrangement (30) of Scheme 11 reveals that the aza-allene **35** is more stable by 19.7 kcal/mol than aminoacetylene **33**. Scheme 12 shows that isomers **13b** and **13c** (Fig. 11) are more stable by 10.7 and 3.7 kcal/mol, respectively, than **13a**, which indicates that there is somewhat more chance to use **13a** as a suitable compound for a Bergman cyclization as in the case of **9a**.

4. Chemical relevance of results

Enediynes are by their electronic nature unstable molecules, which in nature are incorporated into a larger molecular system to prevent their reaction or rearrangement under normal conditions. Bergman cyclization of an enediyne has to be triggered in the special environment of the tumor cell, but when it is triggered its reaction barrier must be low enough to guarantee cyclization at 310 K (body temperature). Hence, instability of the enediyne is a necessary prerequisite to the formation of a similarly labile biradical, which is responsible for the biological activity of the enediynes, possible under the conditions of a tumor cell. Any strong stabilization of an enediyne by either π-delocalization, the formation of more stable CN triple bonds, additional charge delocalization, etc. as observed for enediynes **3**, **7**, **11** and their protonated counterparts **5**, **9**, and **13** reduces their potential as a starting point for a new antitumor drug. Incorporation of these molecules into a 9- or 10-membered ring as is the case of the naturally occurring enediynes will not change the stability situation significantly. In addition, calculations show that **7** upon protonation to yield **9** will easily rearrange to isomer **9b**, which is 34 kcal/mol more stable and can no longer undergo Bergman cyclization. The same is true for **11** and its protonated analog **13** so that the pairs **3**/**5**, **7**/**9**, and **11**/**13** have to be excluded as alternatives to the parent compound **1**, which is contained in most naturally occurring enediynes.

Aza-endiyne **2**, amide **6**, and amidine **10** are destabilized relative to **1** by 7, 18, and 15 kcal/mol, respectively, which is mainly due to a reduction of π-delocalization. Hence, one could argue that **6** or **10** are the most likely candidates for a starting point in the design of a new antitumor drug. On the other hand, one has to consider that actually Bergman cyclization has to take place after protonation in the weakly acidic medium of the tumor cell. The calculated PA values indicate that both aza-enediyne **2** and amide **6** are far too weak as a base to be protonated under weak acidic conditions. Even if one considers that protonation in the cell takes place in an aqueous solution and, therefore, solvation effects will play an important role, the known pK_A values of amides (close to 0 [49]) give little hope that an amide such as **6** provides a promising basis for a new antitumor drug. However, pK_A values of amidines [50,51] describe the latter as strong bases in line with the PA calculated for **10** in this work. Hence, our future efforts to provide quantum chemical information for the design of new enediyne antitumor drugs will concentrate on amidines such as **10** as a promising starting point.

Acknowledgements

This work was supported by the Swedish Natural Science Research Council (NFR). All calculations were done on the CRAY C90 of the Nationellt Superdatorcentrum (NSC), Linköping, Sweden. The authors thank the NSC for a generous allotment of computer time.

References

[1] D.B. Borders, T.W. Doyle (Eds.), Enediyne Antibiotics as Antitumor Agents Marcel Dekker, New York, 1995.
[2] K.C. Nicolaou, A.L. Smith, Acc. Chem. Res. 25 (1992) 497.
[3] K.C. Nicolaou, W.-M. Dai, Angew. Chem. Int. Ed. Engl. 30 (1991) 1387.
[4] W.K. Pogozelski, T.D. Tullius, Chem. Rev. 98 (1998) 1089.
[5] M.E. Maier, F. Boße, A.J. Niestroj, Eur. J. Org. Chem. 1 (1999) 1.
[6] J.S. Thorson, B. Shen, R.E. Whitwam, W. Liu, Y. Li, J. Ahlert, Bioorg. Chem. 27 (1999) 172.
[7] J. Wisniewski Grimssom, G.U. Gunawardena, D. Klingberg, D. Huang, Tetrahedron 19 (1996) 6453.
[8] A.G. Fallis, Can. J.Chem. 77 (1999) 159.
[9] R.R. Jones, R.G. Bergman, J. Am. Chem. Soc. 94 (1972) 660.
[10] R.G. Bergman, Acc. Chem. Res. 6 (1973) 25.
[11] T.P. Lockhart, P.B. Comita, R.G. Bergman, J. Am. Chem. Soc. 103 (1981) 4082.
[12] T.P. Lockhart, R.G. Bergman, J. Am. Chem. Soc. 103 (1981) 4091.
[13] R. Gleiter, D. Kratz, Angew. Chem., Int. Ed. Engl. 32 (1993) 842.
[14] N.J. Turro, A. Evenzahav, K.C. Nicolaou, Tetrahedron Lett. 35 (1994) 8089.
[15] Y. Kuwatani, I. Ueda, Angew. Chem. Int. Ed. Engl. 34 (1995) 1892.
[16] E. Kraka, D. Cremer, J. Am. Chem. Soc. 116 (1994) 4929.
[17] W.R. Roth, H. Hopf, C. Horn, Chem. Ber. 127 (1994) 1765.
[18] R. Marquardt, A. Balster, W. Sander, E. Kraka, D. Cremer, J.G. Radziszewiski, Angew. Chem. 110 (1998) 1001.
[19] J.H. Hoffner, M.J. Schottelius, D. Feichtinger, P. Chen, J. Am. Chem. Soc. 120 (1998) 376.
[20] N. Koga, K. Morokuma, J. Am. Chem. Soc. 113 (1991) 1907.
[21] P.G. Wenthold, J.A. Paulino, R.R. Squires, J. Am. Chem. Soc. 113 (1991) 7414.
[22] P.G. Wenthold, R.R. Squires, J. Am. Chem. Soc. 116 (1994) 6401.
[23] S.G. Wierschke, J.J. Nash, R.R. Squires, J. Am. Chem. Soc. 115 (1993) 11958.
[24] R. Lindh, B.J. Persson, J. Am. Chem. Soc. 116 (1994) 4963.
[25] R. Lindh, T.J. Lee, A. Berhardsson, B.J. Persson, G. Karlstrm, J. Am. Chem. Soc. 117 (1995) 7186.
[26] C.J. Cramer, J.J. Nash, R.R. Squires, Chem. Phys. Lett. 277 (1997) 311.
[27] C.J. Cramer, S. Debbert, Chem. Phys. Lett. 287 (1998) 320.
[28] C.J. Cramer, J. Am. Chem. Soc. 120 (1998) 6261.
[29] E. Kraka, D. Cremer, J. Am. Chem. Soc. (2000) in press.
[30] P.C. Hariharan, J.A. Pople, Theor. Chim. Acta 28 (1973) 213.
[31] R. Krishnan, M. Frisch, J.A. Pople, Chem. Phys. 72 (1980) 4244.
[32] J. Gräfenstein, A.M. Hjerpe, E. Kraka, D. Cremer, J. Phys. Chem., 104 (2000) 1748.
[33] A.D. Becke, J. Chem. Phys. 98 (1993) 5648.
[34] P.J. Stevens, F.J. Devlin, C.F. Chablowski, M. Frisch, J. Phys. Chem. 98 (1994) 11623.
[35] A.D. Becke, Phys. Rev. A 38 (1988) 3098.
[36] C. Lee, W. Yang, R.G. Parr, Phys. Rev. B 37 (1988) 785.
[37] A.D. Becke, J. Chem. Phys. 88 (1988) 2547.
[38] J.E. Carpenter, F. Weinhold, J. Mol. Struct. (Theochem) 169 (1988) 41.
[39] A.E. Reed, F. Weinhold, J. Chem. Phys. 78 (1983) 4066.
[40] A.E. Reed, L.A. Curtiss, F. Weinhold, Chem. Rev. 88 (1988) 899.
[41] E. Kraka, J. Gräfenstein, J. Gauss, F. Reichel, L. Olsson, Z. Konkoli, Z. He, D. Cremer, COLOGNE 99, Göteborg University, 1999.
[42] M.J. Frisch, G.W. Trucks, H.B. Schlegel, G.E. Scuseria, M.A. Robb, J.R. Cheeseman, V.G. Zakrzewski, J.A. Montgomery, Jr., R.E. Stratmann, J.C. Burant, S. Dapprich, J.M. Millam, A.D. Daniels, K.N. Kudin, M.C. Strain, O. Farkas, J. Tomasi, V. Barone, M. Cossi, R. Cammi, B. Mennucci, C. Pomelli, C. Adamo, S. Clifford, J. Ochterski, G.A. Petersson, P.Y. Ayala, Q. Cui, K. Morokuma, D.K. Malick, A.D. Rabuck, K. Raghavachari, J.B. Foresman, J. Cioslowski, J.V. Ortiz, B.B. Stefanov, G. Liu, A. Liashenko, P. Piskorz, I. Komaromi, R. Gomperts, R.L. Martin, D.J. Fox, T. Keith, M.A. Al-Laham, C.Y. Peng, A. Nanayakkara, C. Gonzalez, M. Challacombe, P.M.W. Gill, B. Johnson, W. Chen, M.W. Wong, J.L. Andres, C. Gonzalez, M. Head-Gordon, E.S. Replogle, J.A. Pople, GAUSSIAN 98, Revision A.3, Gaussian, Inc., Pittsburgh, PA, 1998.
[43] K.C. Nicolaou, G. Zuccarello, Y. Ogawa, E.J. Schweiger, T. Kumazawa, J. Am. Chem. Soc. 110 (1998) 4866.
[44] W.R. Roth, O. Adamczak, R. Breuckmann, H.W. Lennartz, R. Boese, Chem. Ber. 124 (1991) 2499.
[45] S. Benson, L.J. Garland, J. Phys. Chem. 95 (1991) 4915.
[46] The chemistry of functional groups, in: J. Zabicky (Ed.), The Chemistry of Amides, Wiley, New York, 1970.
[47] A.L.L. East, J. Chem. Phys. 108 (1998) 3574 (and references therein).
[48] C. Liang, L.C. Allen, J. Am. Chem. Soc. 113 (1991) 1873.
[49] R.B. Homer, C.D. Johnson, The chemistry of functional groups, in: J. Zabicky (Ed.), The Chemistry of Amides, Wiley, New York, 1970 (chap. 3).
[50] J. Oszczapowicz, in: S. Patai, Z. Rappoport (Eds.), The Chemistry of Functional Groups, The Chemistry of Amidines and Imidates, vol. 2, Wiley, New York, 1991 (chap. 12).
[51] G. Häfelinger, F.K.H. Kuske, in: S. Patai, Z. Rappoport (Eds.), The Chemistry of Functional Groups, The Chemistry of Amidines and Imidates, vol. 2, Wiley, New York, 1991 (chap. 1).